Tunable coloration and luminescence in Mn-Ti codoped nanocrystallized glass

XIAOYUN XU*, YINGYING XING, XIFENG LIU, JIE LUO, HAOJIANG TIAN, WEIQI HUANG
Guangzhou City University of Technology, Guangzhou, 510800, China

Rational incorporation of transition metal dopant into glass has been demonstrated to be a promising strategy for functionalization of glass. However, finely tuning the optical response has been met with limited success. Here, we report that the collaborative strategy by codoping and nanocrystallization is an effective way to tune the optical properties of glass. Mn-Ti doped glass and nanocrystallized glass are fabricated and their structural and spectral studies are performed. The results indicate that Mn and Ti ions can effectively incorporate into the nanocrystals after nanocrystallization. This enables to realize tunable colorization from blue and green to yellow. Furthermore, the wavelength tunable luminescence from yellow to green can also be achieved. The interesting optical response is collaboratively contributed by the rich electronic transitions of the co-doped transitions metal dopants and their selective incorporation into the crystalline domains. The findings are supposed to be general to various transition metal dopant combinations, thus paving an effective way for functionalization of glass.

(Received July 26, 2021; accepted November 24, 2021)

Keywords: Transition metal, Glass, Nanocrystallization, Glass-ceramics, Optical properties

1. Introduction

Transition metal ions are an interest type of dopants and closely associated with many significant applications, including tunable and ultra-short pulse lasers, fiber communication, light emitting diode and biological imaging [1-8]. Thus, rational incorporation of transition metal dopants into glass may generate new optical properties that could exceed the pure undoped glass system. For transition metal dopant, the optical response is mainly involved in the *d-d* electronic transition which is governed by the local chemical environment of the matrix. The glass is characteristic of its amorphous structure and the most popular method to tune the optical response of transition metal ions doped glass is via changing the chemical component of the glass system [9,10]. Despite great success and wide applications have been achieved, it still has great limitation in the tunable range because of the distorted local structure. Another attractive approach is through controllable nanocrystallization of the glass [11,12]. In this case, upon external filed (e.g, heat or laser) triggering, amorphous structure can transform into homogeneous crystalline domains and the transition metal dopants are expected to selectively incorporate into them. Encouragingly, the doping efficiency of transition metal dopants inside the nanocrystalline domains is super high and the formed regular structure is favorable for effectively tuning the optical response. In the past several years, some of transition metals (e.g., Cr^{3+}, Ni^{2+} and Co^{2+}) doped nanocrystallized glass have been fabricated and studied [13-16]. Interestingly, various attractive optical responses such as broadband emission and pulse laser operation have been realized. Based upon above progress, it can be expected that exploration of other transition metal ions doped nanocrystallized glass may enrich the candidate box of the optical materials. Here, we report the synthesis and characterization on the Mn-Ti doped nanocrystallized glass. Mn and Ti ions have been found to be able to effectively incorporate into the nanocrystals. As a result, the tunable coloration and intense luminescence can be realized. The results indicate that the collaborative strategy by nanocrystallization and codoping of transition metal ions in nanocrystallized glass produce an alternative avenue for functionalization of glass.

2. Experimental section

2.1. Methods and synthesis

The glass system of ZnO-Al_2O_3-SiO_2 was employed as the host system and MnO and TiO_2 was selected as the dopant precursor. The analytical reagents of the raw materials (ZnO, Al_2O_3, SiO_2, MnO and TiO_2) were used and the glass was fabricated via melting-quenching method. For details, the raw materials with the total weight of ~50 g were thoroughly mixed in an agate mortar and then melted in the aluminum oxide crucible at 1600 ^oC for 2 hours. The homogeneous melt was quickly cast into the copper plate and pressed with another one to form the

glass. It was then transferred into the furnace at 500 °C and annealed for 24 hours. The nanocrystallized glass samples were fabricated via heat-treatment of the as-made glass sample at various temperatures close to the crystallization temperature for 2 hours. The obtained samples were cut into 5 mm × 5 mm × 1 mm and carefully polished for optical characterizations.

2.2. Characterizations

The thermal properties of glass sample were characterized by differential scanning calorimetry (DSC) measurement which was carried out with a heating rate of 10 K/min at air atmosphere. The phase of samples was investigated by X-ray diffraction (XRD) which was performed on an X-ray diffractometer (Rigaku International Corp. Tokyo, Japan) with Cu Kα1 as the radiation source. The micro-Raman analysis was recorded on a Renishaw InVia spectrometer using a 532 nm laser source. The microstructure was studied by transmission electron microscopy (TEM) which was performed on a JEOL 2010F transmission electron microscope. Optical absorption spectra were measured on a Lambda 900 UV/VIS/NIR spectrometer. The excitation, luminescence spectra and luminescence decay were measured on an Edinburgh Instruments FLS980 spectrometer.

3. Results and discussion

The thermal properties of glass sample were characterized by DSC measurement. Fig. 1 shows the DSC curves of the glass samples with various Mn concentration from 0 to 0.7 mol%. The Ti concentration was fixed to 7 mol%. The glass transition temperatures were calculated to be 743.9, 730.8, 729.8, 731.8, 730.3 and 738.7 °C for the samples doped with 0, 0.05, 0.15, 0.3, 0.5 and 0.7 mol% Mn, respectively. The crystallization temperatures were calculated to be 886.6, 883.1, 883.0, 882.1, 880.3 and 881.1 °C for the samples doped with 0, 0.05, 0.15, 0.3, 0.5 and 0.7 mol% Mn, respectively. Obviously, doping the glass sample with Mn leads to the gradual decrease of the glass transition and crystallization temperature. It was supposed that the dopant may act as the nucleation agent for crystallization. Moreover, the difference between glass transition and crystallization temperature is similar for various samples, indicating the Mn doping does not induce much change in the crystallization behavior of the glass.

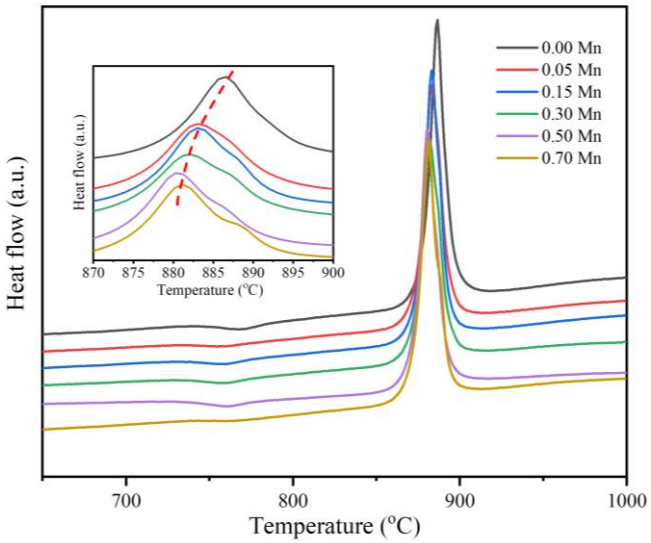

Fig. 1. Thermal properties of glass. DSC curves of glass samples with various Mn concentration. The inset shows the enlarged region between 870 and 900 °C (color online)

The phase and chemical bonding features of samples were studied by XRD. Fig. 2a shows the XRD patterns of as-made and nanocrystallized glass samples heat-treated at various temperatures from 750 to 1000 °C for 2 hours. The as-made and the nanocrystallized sample heat-treated at 750 °C only exhibit a broad halo at ~30 ° and no obvious diffraction pattern can be observed, indicating the amorphous feature of the sample. For the nanocrystallized samples heat-treated above 800 °C, several sharp peaks at 31.0, 36.5, 55.6, 59.4 and 65.3 ° can be observed and they are well consistent with the standard diffraction patterns of $ZnAl_2O_4$ (JCPDF Card No. 05-0669) [17]. With the enhancement of the heat-treatment temperature, the diffraction intensity gradually increases and the bandwidth decreases, indicating the increase of the crystallinity and crystal size, respectively. Fig. 2b exhibits the Raman scattering spectra of the as-made and nanocrystallized glass samples heat-treated at various temperatures from 750 to 1000 °C for 2 hours. The broad band at 920 cm^{-1} can be ascribed to the various vibration modes such as bending and stretching vibrations of SiO_4 tetrahedra [18,19]. With the increase of the heat-treatment temperature, several new bands at ~666.9 and 796.9 cm^{-1} gradually appears. They are originated from the characteristic vibrations of $ZnAl_2O_4$, thus further demonstrating the precipitation of $ZnAl_2O_4$ nanocrystal domains inside the glass [20]. The microstructures of the nanocrystallized glass was further characterized by TEM. Fig. 3 exhibits the typical images of the sample heat-treated at 900 °C for 2 hours. It can be observed that the nanocrystals with the average size of ~8 nm are homogeneously distributed inside the glass matrix (Fig. 3a). Although the size of the crystalline domains is rather

small, the lattice fringe of the nanocrystal is prominent, confirming the excellent crystallinity of the sample. Fig. 3b shows the high resolution TEM image of a single particle and the lattice fringe is estimated to be ~0.2849 nm. It can be ascribed to the *d*(220) spacing of $ZnAl_2O_4$. The results further confirm the precipitation of $ZnAl_2O_4$ nanocrystal domains inside the crystallized glass. The selected area electron diffraction (Fig. 3c) and energy spectrum analysis (Fig. 3d) further confirm the precipitation of the $ZnAl_2O_4$ crystalline phase.

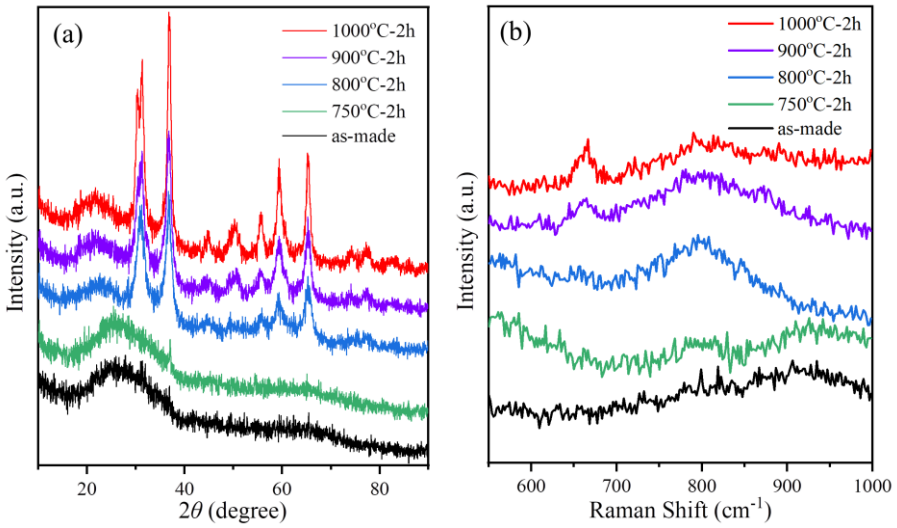

Fig. 2. Phase and chemical bonding features of the nanocrystallized glass. (a, b) XRD (a) and Raman scattering (b) spectra of as-made glass and nanocrystallized glass samples heat-treated at 750, 800, 900 and 1000 °C for 2 hours (color online)

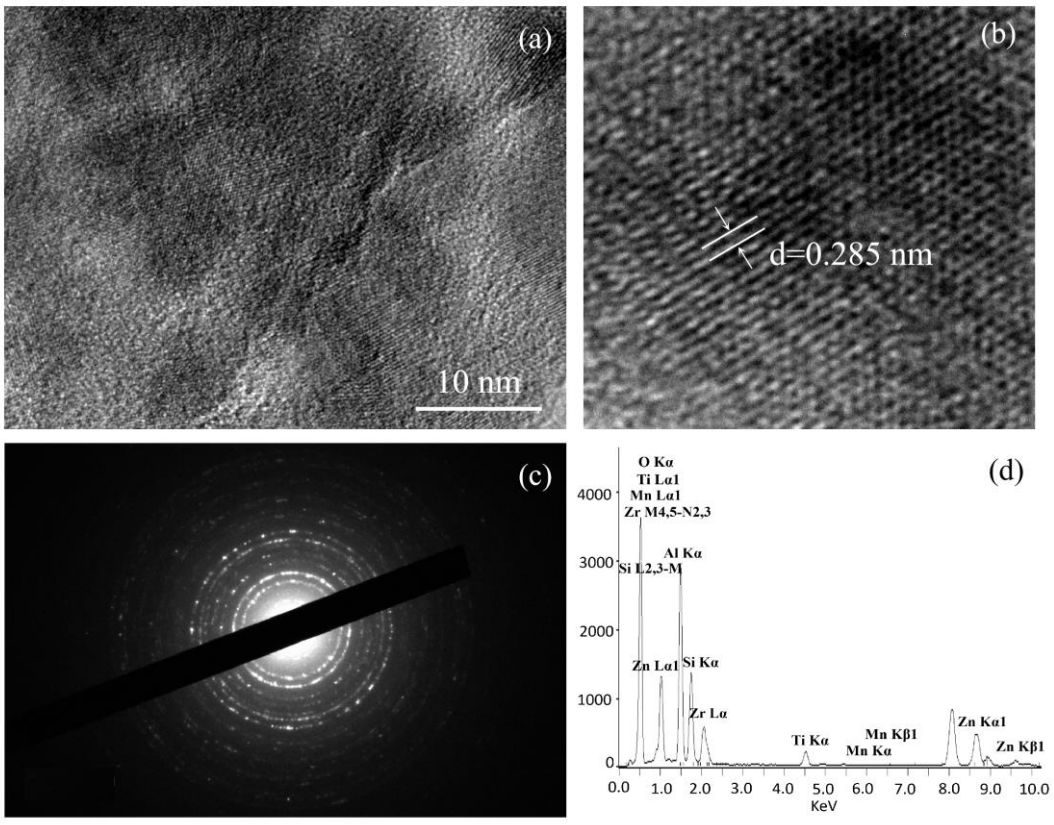

Fig. 3. Microstructures of the nanocrystallized glass. (a, b) TEM (a) and high-resolution TEM image of the nanocrystallized glass samples heat-treated at 900 for 2 hours. (c, d) The selected area electron diffraction (c) and energy spectrum analysis (d) of the nanocrystallized glass samples heat-treated at 900 for 2 hours

Collaborative treatment via Mn and Ti co-doping and nanocrystallization leads to notable change of the appearance of the samples. Fig. 4 exhibits the pictures of the as-made nanocrystallized glass samples doped with different mole ration of Mn. For samples without heat-treatment and treated at relatively low temperature (700 ^{o}C), no obvious colorization can be observed even after doped with high mole ratio Mn (0.7 mol%). Interestingly, nanocrystallization leads to the obvious colorization of samples. For nanocrystallized samples with only Ti doping, heat-treatment induces the appearance of dark blue color. Further incorporation of Mn into Ti-doped nanocrystallized sample results in the notable color change from dark blue to green (0.05-0.15 mol%) and even to yellow color (0.3-0.7 mol%).

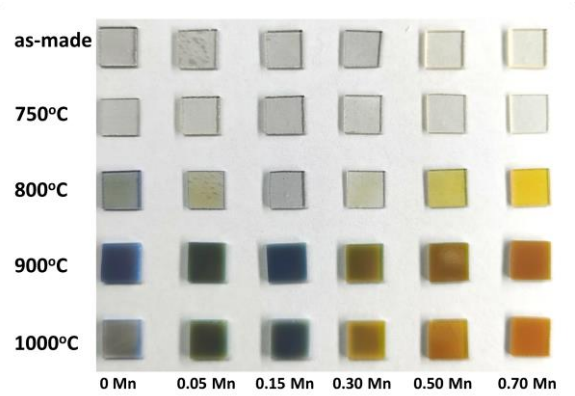

Fig. 4. Appearance of the nanocrystallized glass. Photographs of Ti and Ti-Mn codoped as-made and nanocrystallized samples (color online)

One of the prominent feature of transition metal dopant is that its optical response is sensitive to the local chemical environment. It can be understood by using the Tanabe-Sugano diagram of transition metal dopant. Fig. 5a exhibits the Tanabe-Sugano diagram of Mn^{2+} [21]. It can be seen that the energy gap between various levels are dependent on the crystal field strength, which is determined by the local chemical environment. Thus it can be supposed that the origin of tunable colorization is associated with the local structure change of glass and it was studied by using absorption spectra. Fig. 5b shows the absorption spectra of Ti doped and Ti-Mn co-doped as-made glass samples. The broadband absorption in the ultraviolet-visible range can be attributed to the $^{2}T_{2}\rightarrow{}^{2}E$ transition of Ti^{3+} dopant and the valence-conduction band transition of glass. The absorption in the near-infrared waveband region might be associated with the charge transfer of Ti^{3+} and Ti^{4+} centers, which is frequently observed in Ti-doped glass especially in heavily doped one [22-24]. Further incorporation of Mn into Ti-doped as-made glass leads to the red shift of the absorption; This is mainly resultant from the $^{6}A_{1g}(^{6}S)\rightarrow{}^{4}A_{1g}$,$^{4}E_{g}$, $^{6}A_{1g}(^{6}S)\rightarrow{}^{4}T_{2g}$, and $^{6}A_{1g}(^{6}S)\rightarrow{}^{4}T_{1g}$ transition of Mn^{2+} [25]. Notably, nanocrystallization induces great changes of the absorption spectra (Fig. 5c-f), which is especially prominent in the samples heat-treated above 900 ^{o}C (Fig. 5d). The great increase in the absorption at the wavelength in the range of 350-500 nm is probably associated with the ordering of the local structure around Mn^{2+}, which is favorable for enhancement of the probability of electronic transitions; The phenomenon provides additional evidence about the selective doping of Mn^{2+} inside the crystalline domains inside the nanocrystallized sample. Additionally, the absorption in the red and infrared region centered at ~900 nm is also greatly increased after occurrence of nanocrystallization. The physical origin of this band is still controversial and it has been previously ascribed to the Ti^{3+} ions at interstitial/defect sites and pairs of Ti^{3+}-Ti^{4+} [22-24]. In our case, it is supposed that it is originated from the Ti^{3+}-Ti^{4+} centers because Ti^{3+} and Ti^{4+} centers are frequently observed in glass and nanocrystallization is expected to enhance their interaction such as charge transfer. Thus, the local structure change and the interactions between transition metal dopants collaboratively contributes to the tunable colorization in nanocrystallized glass. The process is summarized by the mechanism diagram shown in Fig. 6.

The nanocrystallization of glass also helps to generate interesting luminescence phenomenon. As shown in the inset of Fig. 6a, as-made glass (the first) and the sample without nanocrystallization (the second) exhibits intense yellow luminescence under excitation with the ultraviolet light (254 nm). The steady luminescence spectrum was employed to studied the emission features and the results are exhibited in Fig. 7a. The excitation spectra are characteristic of broadband excitation bands at ultra-violet region of 250-350 nm, which is originated from the O^{2-}-Mn^{2+} charge transfer. The luminescence spectra is featured by a broad band at 450-800 nm region, which can be ascribed to the $^{4}T_{1g}(4G)\rightarrow{}^{6}A_{1g}(^{6}S)$ electronic transition of Mn^{2+}. Obviously, the nanocrystallization leads to the great shift of the central wavelength of the emission from 600 to 505 nm. Moreover, the bandwidth of the emission also decreases. The great decrease in the spectral bandwidth is mainly resultant from the selective incorporation of Mn^{2+} inside the nanocrystalline phase after nanocrytallization. The luminescence dynamics was studied and the corresponding decay curves are shown in Fig. 7b. It can be observed that the decay curves can not be fitted to the simple exponential function. The average decay lifetime was calculated to be 4.9, 4.8, 15.2, 18.1 and 20.4 μs for the as-made and nanocrystallized glass heat-treated at 750, 800, 900 and 1000 ^{o}C, respectively. The extension of the lifetime after nanocrystallization can be ascribed to the selective incorporation of the transition metal dopants inside the crystalline domains, whose regular environment is favorable for radiation transition.

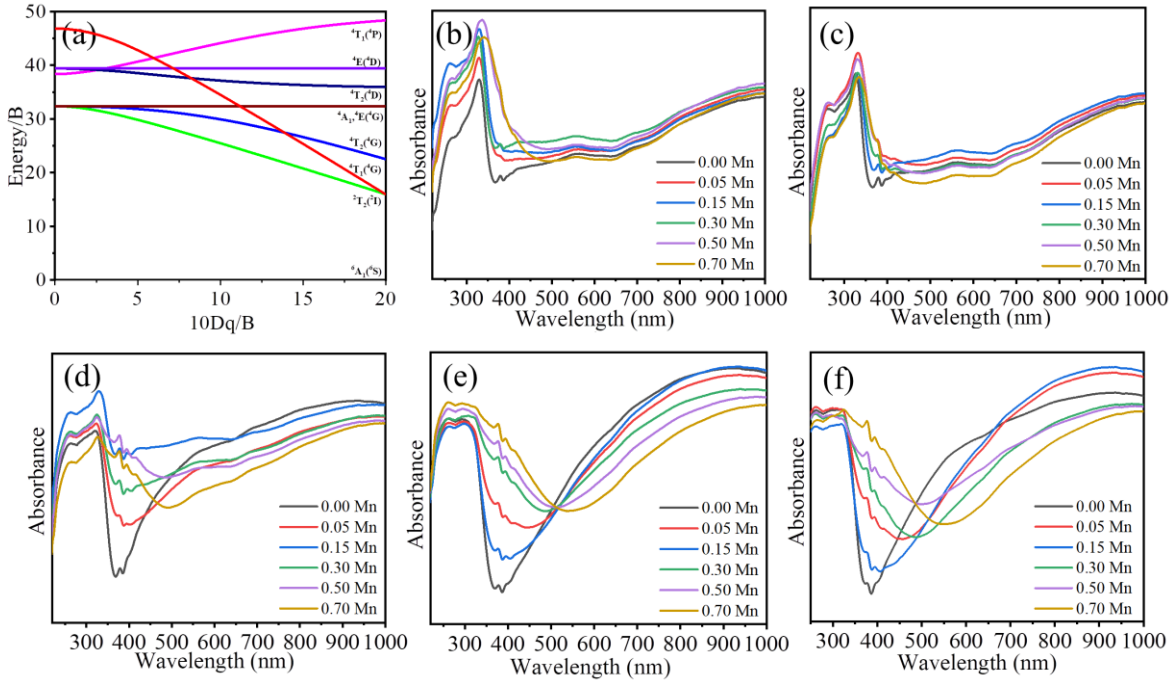

Fig. 5. Absorption feature of the nanocrystallized glass. (a) Tanabe-Sugano diagram of Mn^{2+}. (b) Absorption spectra of Ti doped and Mn-Ti codoped as-made glass (b) and nanocrystallized samples heat-treated at 750 °C (c), 800 °C (d), 900 °C (e) and 1000 °C (f) (color online)

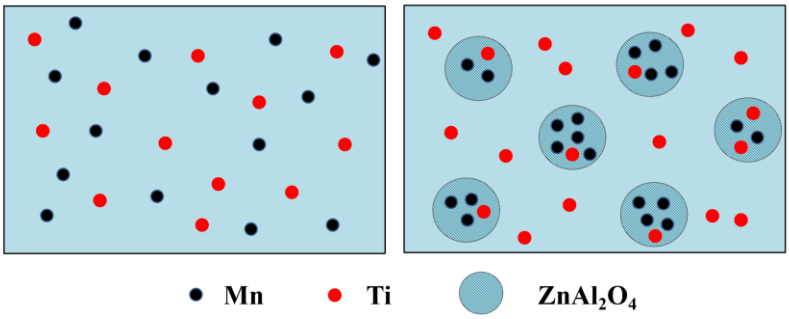

Fig. 6. The mechanism diagram for illustration of the selective doping process of dopants in the nanocrystallized glass. The left part is the glass and the right part is the nanocrystallized glass (color online)

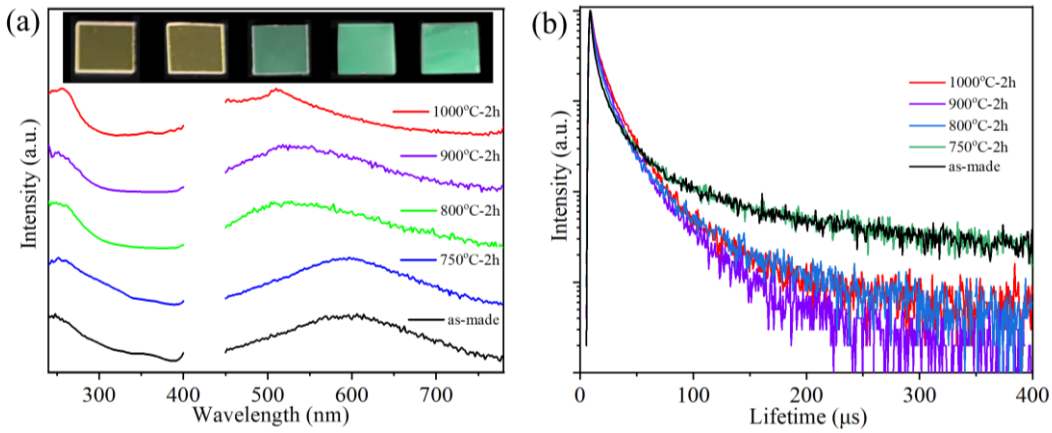

Fig. 7. Luminescence properties of the nanocrystallized glass. (a) Excitation and luminescence spectra of 0.5 mol% Mn doped as-made and nanocrystallized glass heat-treated at 750 °C (c), 800 °C (d), 900 °C (e) and 1000 °C. (b) Decay curves of 0.5 mol% Mn doped as-made and nanocrystallized glass heat-treated at 750 °C (c), 800 °C (d), 900 °C (e) and 1000 °C (color online)

4. Conclusions

In summary, we have designed and fabricated Mn-Ti codoped nanocrystallized glass. The structural and optical characterizations show that the nanocrystallization of glass and precipitation of $ZnAl_2O_4$ crystalline phase enables to realize tunable colorization from blue and green to yellow. Furthermore, the wavelength tunable luminescence from yellow to green can be achieved. The physical mechanism has been discussed and the interesting optical phenomenon is collaboratively contributed by the rich electronic transitions of the Mn-Ti dopants and their selective incorporation into the $ZnAl_2O_4$ crystalline domains. The results not only represent the first studies on the Mn-Ti codoped nanocrystallized glass but also provide a new avenue for functionalization of glass. Furthermore, the strategy is supposed to be general to various different types of transition metal dopant combinations.

Acknowledgments

We gratefully acknowledge the financial support from National Natural Science Foundation of China (12104163), the Department of Education of Guangdong Province (2020KTSCX202), the Fund for Art & Design in Guangzhou City University of Technology (60-CQ190025) and the Open Fund of Key Laboratory of Electromagnetic Transformation and Detection (Luoyang Normal University).

References

[1] S. Kück, Appl. Phys. B **72**, 515 (2001).
[2] S. C. Erwin, L. J. Zu, M. I. Haftel, A. L. Efros, T. A. Kennedy, D. J. Norris, Nature **436**, 91 (2005).
[3] N. Vivet, M. Morales, M. Levalois, J. L. Doualan, R. Moncorge, Appl. Phys. Lett. **90**, 181915 (2007).
[4] S. Zhou, C. Li, G. Yang, G. Bi, B. Xu, Z. Hong, K. Miura, K. Hirao, J. Qiu, Adv. Funct. Mater. **23**, 5436 (2013).
[5] Y. Yu, F. Huang, D. Chen, H. Lin, R. Zhang, A. Yang, K. Li, Y. Wang, Laser Phys. **24**, 025101 (2014).
[6] L. Lin, Y. Wang, B. Lan, J. Chen, S. Lv, Y. Zhao, H. Yu, J. Hao, Q. Zhang, Z. Yang, H. Zhang, J. Wang, J. Qiu, S. Zhou, J. Phys. Chem. C **123**, 29343 (2019).
[7] Y. Zhang, X. Li, Z. Lai, R. Zhang, E. Lewis, A. I. Azmi, Z. Gao, X. Lu, Y. Chu, Y. Liu, Q. Chai, S. Sun, J. Ren, J. Zhang, J. Phys. Chem. C **123**, 10021 (2019).
[8] L. Cormier, S. Zhou, Appl. Phys. Lett. **116**, 260503 (2020).
[9] M. A. Bunuel, J. Garcia, M. G. Proietti, J. A. Solera, R. Cases, J. Chem. Phys. **110**, 3566 (1999).
[10] L. Galoisy, L. Cormier, G. Calas, V. Briois, J. Non-Cryst. Solids **293**, 105 (2001).
[11] O. Dymshits, M. Shepilov, A. Zhilin, MRS Bull. **42**, 200 (2017).
[12] X. Liu, J. Zhou, S. Zhou, Y. Yue, J. Qiu, Prog. Mater. Sci. **97**, 38 (2018).
[13] B. N. Samson, L. R. Pinckney, J. Wang, G. H. Beall, N. F. Borrelli, Opt. Lett. **27**, 1309 (2002).
[14] A. Goldstein, P. Loiko, Z. Burshtein, N. Skoptsov, I. Glazunov, E. Galun, N. Kuleshov, K. Yumashev, J. Am. Ceram. Soc. **99**, 1324 (2016).
[15] J. Chen, Z. Shi, S. Zhou, Z. Fang, S. Lv, H. Yu, J. Hao, H. Zhang, J. Wang, J. Qiu, Adv. Opt. Mater. **7**, 1801413 (2019).
[16] J. Ren, X. Lu, C. Lin, R. Jain, Opt. Express **28**, 21522 (2020).
[17] T. Suzuki, K. Horibuchi, Y. Ohishi, J. Non-Cryst. Solids **351**, 2304 (2005).
[18] Y. Huang, Z. Jiang, W. Schwieger, Chem. Mater. **11**, 1210 (1999).
[19] B. G. Parkinson, D. Holland, M. E. Smith, C. Larson, J. Doerr, M. Affatigato, S. A. Feller, A. P. Feller, A. P. Howes, C. R. Scales, J. Non-Cryst. Solids **354**, 1936 (2008).
[20] D. Simeone, C. Dodane-Thiriet, D. Gosset, P. Daniel, M. Beauvy, J. Nucl. Mater. **300**, 151 (2002).
[21] Y. Tanabe, S. Sugano, J. Phys. Soc. Jpn. **9**, 766 (1954).
[22] H. Liu, F. Gan, J. Non-Cryst. Solids **80**, 422 (1986).
[23] P. F. Moulton, J. G. Cederberg, K. T. Stevens, G. Foundos, M. Koselja, J. Preclikova, Opt. Mater. Express **9**, 2216 (2019).
[24] L. H. C. Andrade, S. M. Lima, A. Novatski, P. T. Udo, N. G. C. Astrath, A. N. Medina, A. C. Bento, M. L. Baesso, Y. Guyot, G. Boulon, Phys. Rev. Lett. **100**, 027402 (2008).
[25] R. Ye, G. Jia, D. Deng, Y. Hua, Z. Cui, S. Zhao, L. Huang, H. Wang, C. Li, S. Xu, J. Phys. Chem. C **115**, 10851 (2011).

*Corresponding author: xuxiaoyun@gcu.edu.cn